MEASUREMENT AND MODELING ON HYDROGEN JET AND COMBUSTION FROM A PRESSURIZED VESSEL

Ba, Q.X.[1], Xiao, J.J.[2], Jordan, T.[2], Huang, T.[1], Zhao, M.B.[1], Xiao, G.P.[3,*], Li, X.F.[1,*]
[1] Institute of Thermal Science and Technology, Shandong University, Jinan 250061, China
[2] Institute for Thermal Energy Technology and Safety, Karlsruhe Institute of Technology, Eggenstein-Leopoldshafen, 76344, Germany
[3] Shanghai Institute of Applied Physics, Chinese Academy of Sciences, Shanghai 201800, China
*** Corresponding authors: xiaoguoping@sinap.ac.cn, lixf@email.sdu.edu.cn**

ABSTRACT

Hydrogen safety is an important topic for hydrogen energy application. Unintended hydrogen releases and combustions are potential accident scenarios, which are of great interest for developing and updating the safety codes and standards. In this paper, hydrogen releases and delayed ignitions were studied. The hydrogen was released from a pressurized vessel to atmosphere through a 4 mm inner diameter circular nozzle and then ignited at 40 cm away from the nozzle. The pressurized vessel volume was 2.815 L with the initial pressure of 5 bar and temperature of 293 K. The hydrogen was ignited at 80 ms after the leakage. The pressure decreases in the vessel were measured. The leakage and flame propagation processes were visualized by a high speed camera. Then, the hydrogen leakage and combustion processes were modelled using the parallel CFD code GASFLOW-MPI. The k-ε model was used for the turbulence and the eddy dissipation model (EDM) was used for the combustion.The predicted hydrogen flame propagations agreed with the experimental results. The flame spread forward immediately after the ignition and spread back to the nozzle at 20 ms after ignition. The calculated flame temperature distributions agreed well with the schlieren images. The pressure field was also calculated. The calculated overpressure expanded from the ignition point to surrounding areas and gradually decreased. The maximum overpressure after ignition was 5.5 kPa, occurring at the ignition location.

KEYWORDS: hydrogen safety, release, delayed ignition, flame propagation, GASFLOW-MPI

1 INTRODUCTION

As a promising clean and sustainable energy carrier, hydrogen has been increasingly used in recent years, which can help relieve the fossil fuel crisis and air pollution [1-3]. Hydrogen is a flammable gas that has wide flammability limits in air and a high flame speed. Therefore, hydrogen safety is an important topic for hydrogen energy application. Reliable safety codes and standards are needed in hydrogen production, pipeline delivery, road transport, storage, and use to prompt the hydrogen commercialization.

Hydrogen is usually stored at high pressures due to its low volumetric energy density. Unintended hydrogen releases and ignitions are potential accident scenarios, which are of great interest for developing and updating the safety codes and standards. Many studies have measured the hydrogen jet flames resulting from underexpanded jets [4-6]. The flame lengths and widths from circular nozzles were determined from the storage pressure and nozzle diameter [5]. The empirical correlations for the flame length and width were obtained [4, 5]. The hydrogen jet flames have also been numerically modeled using Computational Fluid Dynamics (CFD) methods to predict the temperature distributions [7, 8].

Existing studies mainly focus on the hydrogen jet flames after the fire stabilized. The flame propagation and development processes have not been well studied. A complex interaction between turbulence, chemical reaction and ignition parameters determines the flame development and propagation after ignition. Veser [9] and Friedrich et al. [10] carried out ignition experiments for room temperature and cryogenic hydrogen jets. The flame propagations were observed using a Background Oriented Schlieren (BOS) system. Depending on the ignition location three different flame modes

were identified: ignition flash-back to the nozzle followed by a stable jet flame, stable lifted flame without flash-back, and unstable transient flame with quenching. The thresholds of the hydrogen concentration between the three flame propagation regimes are 11% and 5% correspond to the distance from the nozzle. In the experiment, the hydrogen mass flow rate remained stable during the leakage. However, when hydrogen releases from a pressurized vessel with a given volume, the stagnation state and mass flow rate change with time. Therefore, the stagnation state time histories and the flame propagations need to be further studied for the release and ignition of hydrogen stored in a pressurized vessel.

In addition, previous experiments have not measured the temperature and overpressure distributions. Ignition of the hydrogen jet may cause high temperature and overpressure, which will damage the measuring sensors. Therefore, numerical modeling for hydrogen release and ignition is necessary to predict the temperature and pressure distributions.

In this paper, the hydrogen release and combustion were studied for hydrogen released from a pressurized vessel to atmosphere through a circular nozzle and then ignited at 40 cm away from the nozzle. The nozzle had a 4 mm inner diameter. The pressurized vessel volume was 2.815 L with the initial pressure of 5 bar and temperature of 293 K. The hydrogen was ignited at 80 ms after the leakage. The pressure decreases in the vessel were measured. The leakage and flame propagation processes were visualized by a BOS system.Then, the hydrogen leakage and combustion processes were modelled using the parallel CFD code GASFLOW-MPI. The hydrogen flame propagations were reproduced and the overpressure field was predicted.

2 EXPERIMENTAL FACILITY

The experimental investigation of hydrogen release and combustion was carried out with the DisCha-facility at Karlsruhe Institute of Technology (KIT). The DisCha facility mainly consisted of a stainless steel pressure vessel with an internal free volume of 2.815 L and a weight of about 28 kg, as shown in Fig. 1. The vessel was equipped with several ports for instrumentation on its top and a rod that points on a force sensor on its rear side. Opposite to the force sensor a tubular exhaust pipe was welded to the vessel, where release nozzles with different aperture sizes can be fastened. A nozzle with an inner diameter of 4 mm was used in this experiment. The nozzle was 1 m above the ground.

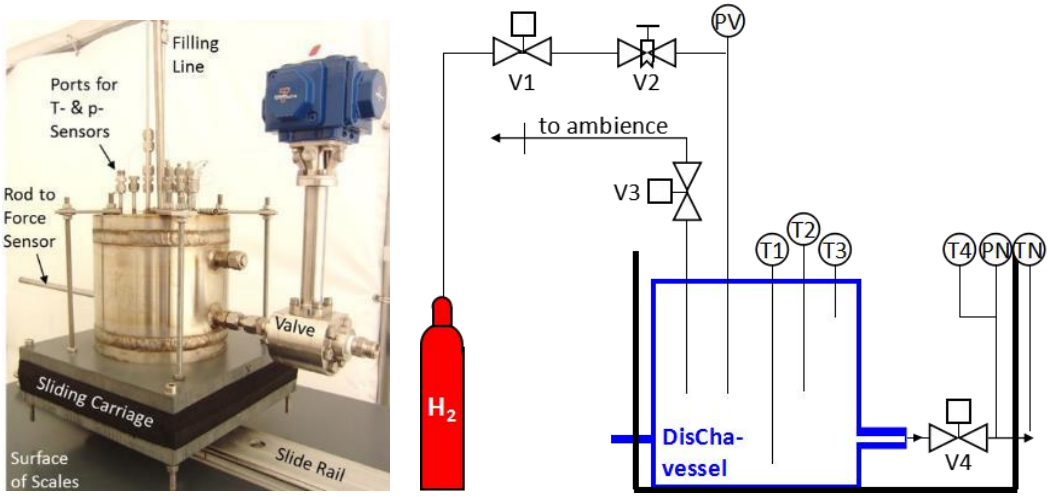

Fig. 1 Experiment system.

One static pressure sensor (PV in Fig. 1) in the filling line was used to control the initial pressure inside the vessel during the filling procedure and capture the pressure decrease inside the vessel during the experiment. A second pressure sensor (PN in Fig. 1) measured the pressure changes in the release line. Since the second sensor was connected to the tube in between the release valve and the nozzle, the first increase in this signal corresponds to the actual start of the release. NiCr/Ni-thermocouples

(Type K, diameter 0.36 mm) were installed inside the vessel to record the gas temperature during the experiment at different heights. The Background Oriented Schlieren (BOS) technique was used to monitor the hydrogen jets and flame propagations. The BOS technique was based on the optical deformation of a background pattern due to density gradients in the gas system under investigation, which was described in [11]. The method was similar to the Schlieren technique and effective for gases with a prominent density difference like hydrogen jet into air and for combustion processes. A CCD camera was used to record the images followed by digital image processing.

The initial vessel pressure was 5 bar with a temperature of 293 K. The hydrogen was released from the nozzle and then ignited at 80 ms after the leakage. The ignition point was at 40 cm away from the nozzle.

3. NUMERICAL MODELS

GASFLOW-MPI is a parallel CFD code developed at KIT and has been validated for predicting transport, mixing, and combustion of hydrogen and other gases [12-14]. Implicit Continuous Eulerian-Arbitrary Lagrangian-Eulerian solution algorithm (ICE'd ALE) is used in GASFLOW-MPI to solve the three dimensional compressible Navier-Stokes equations. The Arbitrary-Lagrangian-Eulerian (ALE) technique is applicable to flows from supersonic to the incompressible limit [15].

3.1 Turbulence Model

The k-ε turbulence model was used. The turbulence kinetic energy, k, and its rate of dissipation, ε, are obtained from the following transport equations

$$\frac{\partial(\rho k)}{\partial t} + \nabla \cdot (\rho k \boldsymbol{u}) = \nabla \cdot \left[\left(\mu_l + \frac{\mu_t}{\sigma_k} \right) \nabla k \right] + P_k + P_{kb} - \rho \varepsilon \tag{1}$$

$$\frac{\partial(\rho \varepsilon)}{\partial t} + \nabla \cdot (\rho \varepsilon \boldsymbol{u}) = \nabla \cdot \left[\left(\mu_l + \frac{\mu_t}{\sigma_\varepsilon} \right) \nabla \varepsilon \right] + C_{\varepsilon 1} \frac{\varepsilon}{k} (P_k + P_{kb}) - C_{\varepsilon 2\rho} \frac{\varepsilon^2}{k} \tag{2}$$

where ρ is the density, $\boldsymbol{u}$ is the velocity, t is time, μ_l is the molecular viscosity and the turbulent viscosity, μ_t, can be written as [16]

$$\mu_t = C_\mu \rho k^2 / \varepsilon \tag{3}$$

P_k is the turbulence generation due to the viscous forces calculated as

$$P_k = -\frac{2}{3} \rho k \nabla \cdot \boldsymbol{u} - \frac{2}{3} \mu_t (\nabla \cdot \boldsymbol{u})^2 + \mu_t \nabla \boldsymbol{u} \cdot (\nabla \boldsymbol{u} + (\nabla \boldsymbol{u})^T) \tag{4}$$

P_{kb} is the turbulence production term due to the buoyancy calculated as

$$P_{kb} = -\frac{\mu_t}{\sigma_b} g \cdot \nabla \rho \tag{5}$$

The constants in the k-ε model $C_{\varepsilon 1} = 1.44$, $C_{\varepsilon 2} = 1.92$, $C_\mu = 0.09$, $\sigma_k = 1.0$, $\sigma_\varepsilon = 1.3$.

3.2 Combustion Model

A simple one-step global chemical kinetics model was used, which simplifies the actual chemical processes [17]. In the present implementation of this model, the only reaction modeled is $2\mathrm{H_2} + \mathrm{O_2} \rightarrow \mathrm{H_2O}$.

The transport equation of the density-weighted mean reaction progress variable is solved to model the flame front propagation.

$$\frac{\partial(\rho\xi)}{\partial t}+\nabla\cdot(\rho\xi\boldsymbol{u})=\nabla\cdot\left[\left(\mu_l+\frac{\mu_t}{Sc_t}\right)\nabla\xi\right]+\rho S_\xi \tag{6}$$

where Sc_t is the turbulent Schmidt number, ξ is the reaction progress variable, which is 1 in the burnt mixture and 0 in the unburnt mixture. The key to this modeling approach is the source term, ρS_ξ. Eddy dissipation model (EDM) is based on the assumption that combustion occurs at small scales, where mixing occurs on a molecular level and the rate is assumed to be proportional to the inverse of the turbulent time scale [18]. It was developed from the original eddy break-up model, where the most significant difference is that the EDM model accounts for the fact that the reaction rate cannot occur unless both fuel and oxidizer mix on a molecular scale at a sufficiently high temperature. This is accomplished by relating the reaction rate to the limiting species. In GASFLOWMPI, the model is written as

$$\rho S_\xi = B_1\rho\frac{\varepsilon}{k}\min\left(\mathrm{Y}_{\mathrm{H_2}},\frac{\mathrm{Y}_{\mathrm{O_2}}}{\varphi},B_2\frac{\mathrm{Y}_{\mathrm{H_2O}}}{1+\varphi}\right) \tag{7}$$

where the model constants B_1 =50 and B_2 = 0.5, Y is the local mass fraction of each species and φ is the equivalence ratio.

3.3 Geometry and Grid

The computational domain is shown in Fig. 2(a). The hydrogen was released from a pressurized vessel through circular nozzle and then ignited at 40 cm away from the nozzle. The hydrogen storage vessel volume was 2.815 L with initial pressure of 5 bar and temperature of 293 K. The nozzle inner diameter was 4 mm, which was enlarged to 7.5 mm for the calculation, mainly considering the computational cost. A sub-grid mass flow rate model was used at the nozzle outlet to ensure the identity with the actual mass flow. A frictionless adiabatic solution for the mass flow rate of hydrogen release is provided as

$$m=\begin{cases} C_d\cdot A\sqrt{\gamma p_1\rho_1\left(\dfrac{2}{\gamma+1}\right)^{\frac{\gamma+1}{\gamma-1}}} & ;\ \dfrac{p_2}{p_1}<\left(\dfrac{2}{\gamma+1}\right)^{\frac{\gamma}{\gamma-1}} \\ C_d\cdot A\sqrt{2p_1\rho_1\left(\dfrac{\gamma}{\gamma-1}\right)\left[\left(\dfrac{p_2}{p_1}\right)^{\frac{2}{\gamma}}-\left(\dfrac{p_2}{p_1}\right)^{\frac{\gamma+1}{\gamma}}\right]} & ;\ \dfrac{p_2}{p_1}\geqslant\left(\dfrac{2}{\gamma+1}\right)^{\frac{\gamma}{\gamma-1}} \end{cases} \tag{8}$$

where A is the computational nozzle area. C_d is the discharge coefficient, which is the ratio of the actual area and computational area and equals to 0.284 in this study. p_1 and ρ_1 are the pressure and hydrogen density in the vessel, p_2 is the ambient pressure, and the specific heat ratio of hydrogen γ=1.4.

The computational domain was discretized using hexahedral elements, with 211×118×211 grids at x, y and z direction. Very fine grids were used around the nozzle exit to ensure convergence and the calculation accuracy as shown in the cross-sectional view of the mesh in Fig. 2(b). The ambient air temperature was 293 K and the ambient pressure was 1.0 bar.

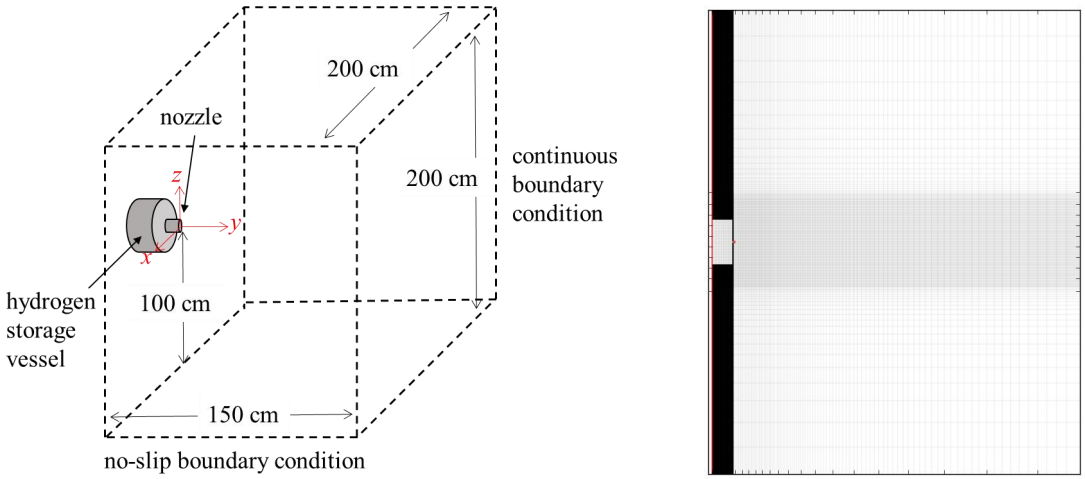

(a) Computational domain (b) Cross-sectional view of the mesh

Fig. 2 Computational domain and mesh.

4. RESULTS AND DISCUSSION

4.1 Hydrogen Release and Distribution before Ignition

The storage vessel pressure dropped from 5 bar to 3.46 bar during the release as shown in Fig. 3, which was well predicted by GASFLOW-MPI. The calculated vessel pressure was 3.30 bar at 80 ms, 4.62% lower than the measured pressure. The error is because that the calculation model ignored the pressure loss from the storage vessel to the nozzle, resulting in a larger hydrogen leakage flow and a faster vessel pressure drop. Measured and calculated hydrogen jets at 80 ms after the leakage are shown in Fig. 4. The hydrogen diffusion regions agree well although the exact concentration values have not been measured by the BOS system. The calculated jet centerline hydrogen mole fractions and velocities at 80 ms are shown in Fig. 5. The distribution of hydrogen mole fraction fluctuated due to the instantaneous turbulent.

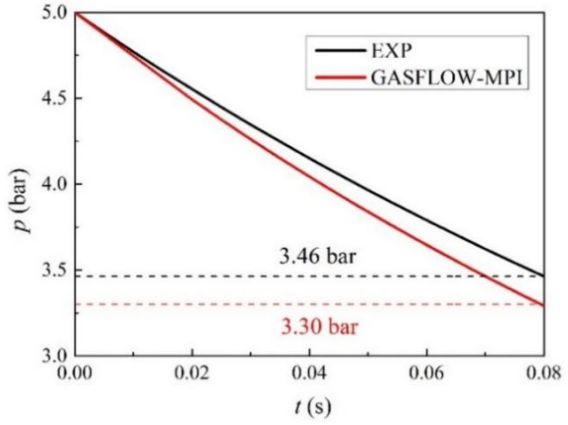

Fig. 3 Storage vessel pressure.

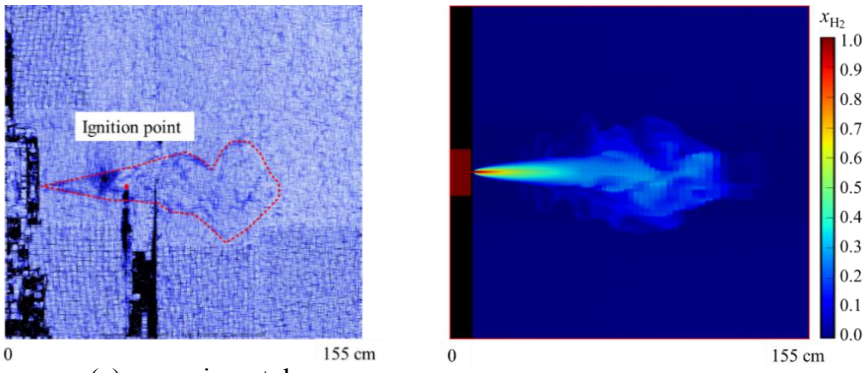

(a) experimental (b) calculated hydrogen volume fraction

Fig. 4 Hydrogen jet at 80 ms after leakage.

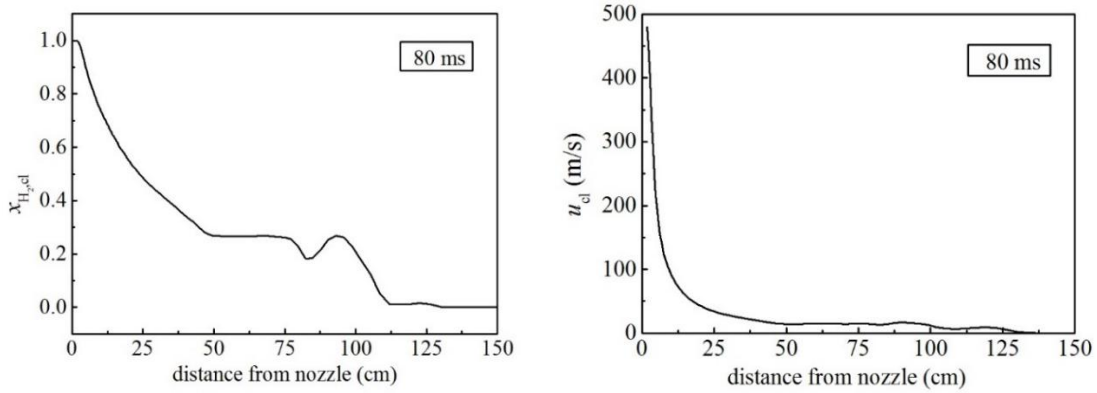

(a) Centerline hydrogen mole fractions (c) Centerline velocities

Fig. 5 Centerline hydrogen mole fractions and velocities at 80 ms.

4.2 Hydrogen Flame Propagations

The hydrogen jet was ignited at 40 cm away from the nozzle at 80 ms after the leakage. The complex interaction of turbulence and chemical reaction determined the further progress of the combustion. A sequence of BOS images and the calculated flame temperature contours are shown in Fig. 6. After ignition at the indicated ignition point, the flame propagated downstream immediately, while at the same time the turbulent flame front moved towards to the nozzle. The calculated flame shape is compared with the BOS image at 20 ms after ignition when the flame spreads back to the nozzle in Fig. 7. The flame propagation processes and shapes in Fig. 6 and Fig. 7 show good agreement between the predicted and measured results. The average downstream flame velocity within 20 ms after ignition was 36.75 m/s. The average upstream flame velocity within 20 ms after ignition was 20 m/s.

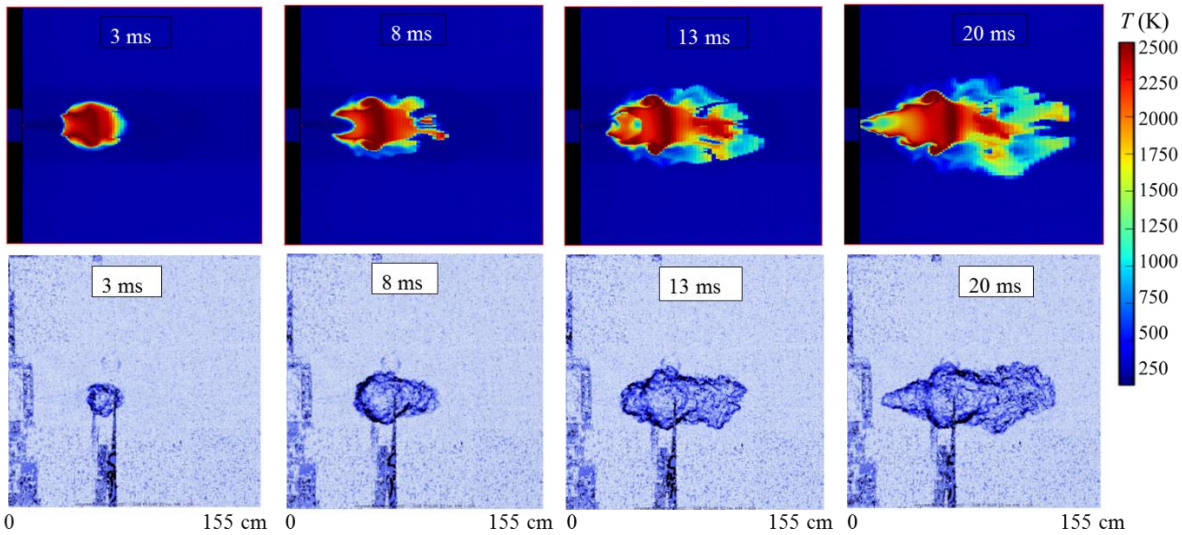

Fig. 6 Flame propagation after ignition (up: GASFLOW-MPI; down: experimental)

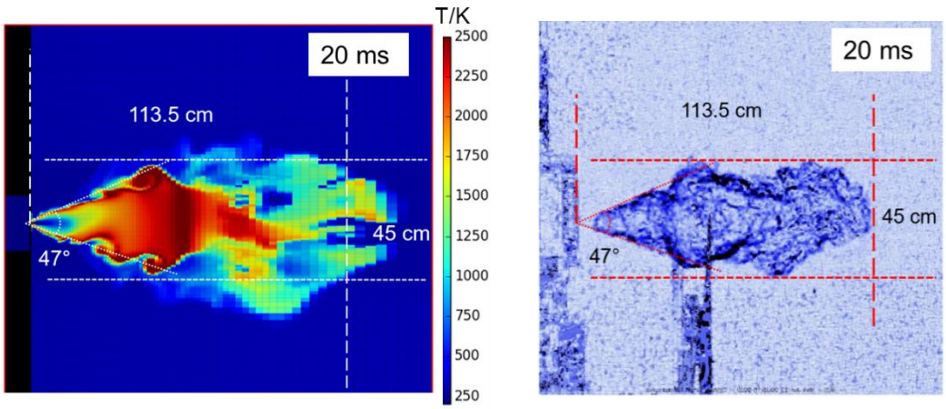

(a) Calculated (b) Experimental

Fig. 7 Experimental and calculated flames at 20 ms after ignition

4.3 Calculated Overpressures

The overpressure expanded from the ignition point to surrounding areas and gradually decreased, as shown in Fig. 8. The transient overpressures along the jet centerline (Line 1, Y1~Y6 in Fig. 9) and the *x*-axis direction (Line 2, X1~X4 in Fig. 9) are shown in Fig. 10. The distances from monitoring points Y1~Y6 to the nozzle outlet were 25 cm, 35 cm, 45 cm, 55 cm, 70 cm and 90 cm. The distances between X1~X4 and the ignition point were 5 cm, 10 cm, 20 cm and 40 cm. The overpressure decayed as the distance from ignition point increases, as shown in Fig. 10. The maximum overpressure was 5.5 kPa, occurring near the ignition location. In Fig. 10(a), the transient overpressures for Y2 and Y3 are almost the same due to the same distance from ignition point, as well as Y1 and Y4.

The maximum overpressures along jet centerline (Line 1) are shown in Fig. 11(a). The black line is the overpressure on the left side of ignition point and the red line is the overpressure on the right side. The maximum overpressure decays with distance from ignition point. However, there is an exception near the nozzle on the left side, where the maximum overpressure increases due to the obstruction of pressure wave by hydrogen storage vessel. The damage limit of overpressure is divided to three levels by European Industrial Gases Association [19], as listed in Table 1. The no harm distance from ignition point is 65 cm along jet direction. The maximum overpressures along Line 2 are shown in Fig. 11(b). The maximum overpressure on both sides of ignition point is symmetric and decays as the distance from ignition point increases. The no harm overpressure distance from ignition point is 67 cm along x-axis direction.

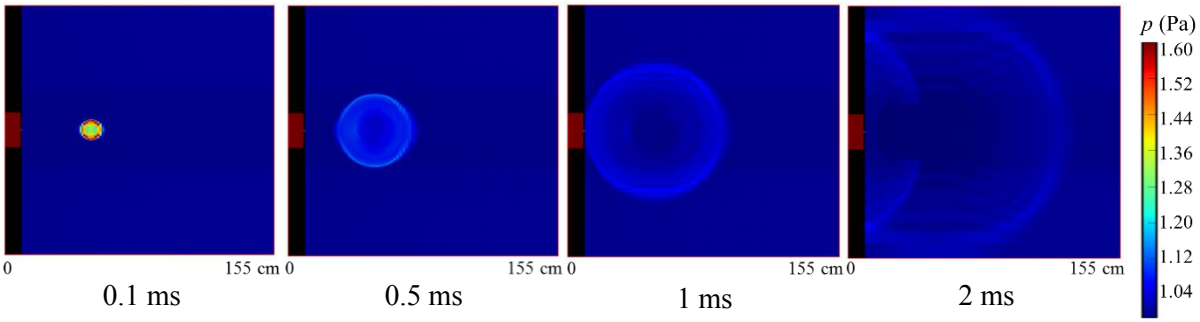

Fig. 8 The calculated pressure field after ignition

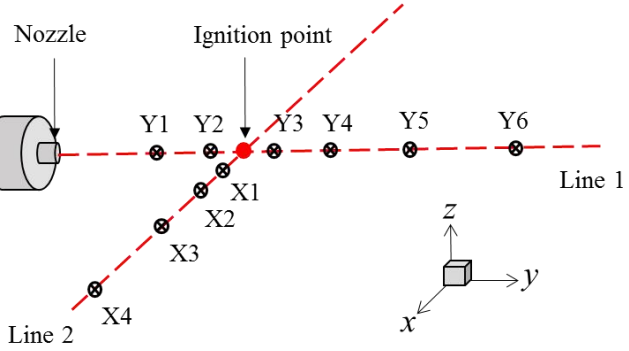

Fig. 9 Overpressure monitoring points

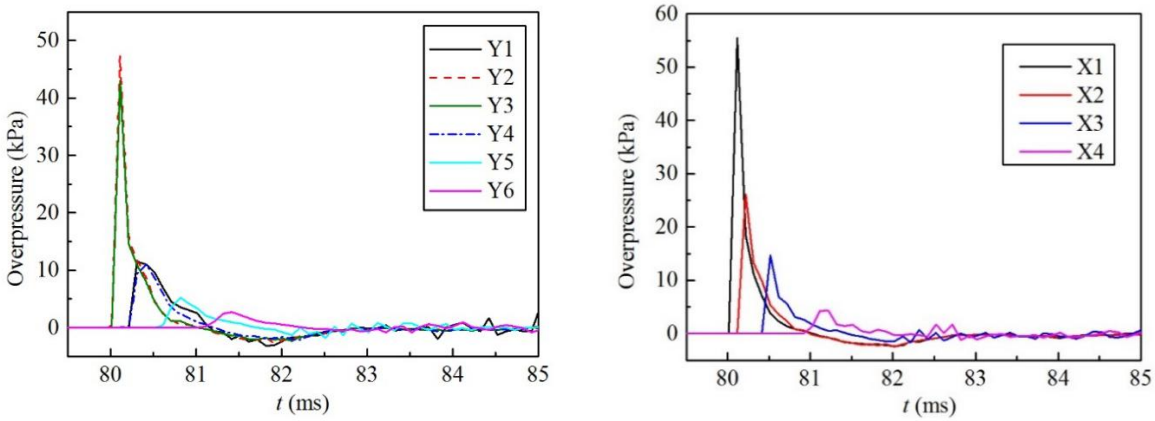

(a) transient overpressures at points Y1~Y6 (b) transient overpressures at points X1~X4

Fig. 10 Transient overpressures at monitoring points

Table 1 Damage limits of overpressure [19]

Overpressure (kPa)	Damage
20	Damage to equipment
7	Harm to people
2	No harm

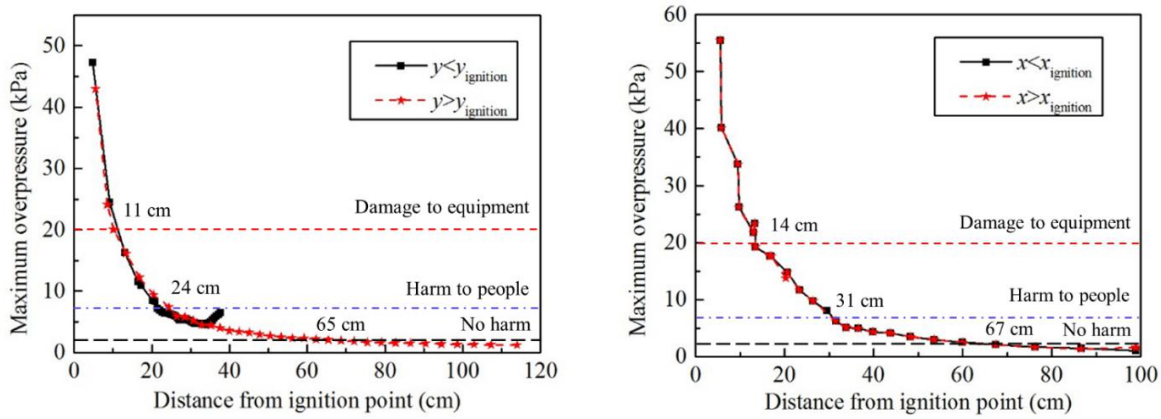

(a) maximum overpressures along Line1 (b) maximum overpressures along Line2

Fig. 11 Maximum overpressures

5. CONCLUSIONS

This study measured and modeled the hydrogen release and ignition processes. The hydrogen storage vessel volume was 2.815 L with initial pressure of 5 bar and temperature of 293 K. The hydrogen was ignited at 40 cm away from a nozzle with 4 mm inner diameter. The CFD models using GASFLOW-MPI solved the three-dimensional, instantaneous Navier-Stokes equations with the k-ε turbulence model and EDM combustion model.

The measured storage vessel pressure dropped from 5 bar to 3.46 bar before ignition, which was well predicted by GASFLOW-MPI. After ignition at the indicated ignition point, the flame propagated downstream immediately, while at the same time the turbulent flame front moved towards to the nozzle. The flame spread back to the nozzle at 20 ms after ignition. The average downstream flame velocity within 20 ms after ignition was measured to be 36.75 m/s, while the average upstream flame velocity within 20 ms after ignition was 20 m/s. The good agreement between the calculated and experimental data confirms the powerful feature of GASFLOW-MPI in the simulation of hydrogen combustion in the free turbulent jet. The overpressure expanded from the ignition point to surrounding areas and gradually decreased. The maximum overpressure was 5.5 kPa, occurring near the ignition location. The no harm overpressure distance was 67 cm from ignition point.

The present results contribute to the evaluation for the accident consequences of hydrogen leakage and combustion.

ACKNOWLEDGMENT

This study was supported by the Youth Innovation Promotion Association of the Chinese Academy of Sciences (2018298), the National Natural Science Foundation of China (No. 51706125) and the Fuel Cells and Hydrogen Joint Undertaking (No. 779613).

REFERENCES

[1] Barbir F., Transition to Renewable Energy Systems with Hydrogen as an Energy Carrier, *Energy*, **34**, No. 3, 2009, pp. 308-312.

[2] Apak S., Atay E. and Tuncer G., Renewable Hydrogen Energy and Energy Efficiency in Turkey in the 21st Century, *International Journal of Hydrogen Energy*, **42**, No. 4, 2017, pp. 2446-2452.

[3] Panwar N. L., Kaushik S. C. and Kothari S., Role of Renewable Energy Sources in Environmental Protection: A Review, *Renewable and Sustainable Energy Reviews*, **15**, No. 3, 2011, pp. 1513-1524.

[4] Schefer R., Houf W. and Bourne B. et al., Spatial and Radiative Properties of an Open-flame Hydrogen Plume, *International Journal of Hydrogen Energy*, **31**, No. 10, 2006, pp. 1332-1340.

[5] Mogi T. and Horiguchi S., Experimental Study on the Hazards of High-pressure Hydrogen Jet Diffusion Flames, *Journal of Loss Prevention in the Process Industries*, **22**, No. 1, 2009, pp. 45-51.

[6] Panda P. P. and Hecht E. S., Ignition and Flame Characteristics of Cryogenic Hydrogen Releases, *International Journal of Hydrogen Energy*, **42**, No. 1, 2017, pp. 775-785.

[7] Brennan S. L., Makarov D. V. and Molkov V., LES of High Pressure Hydrogen Jet Fire, *Journal of Loss Prevention in the Process Industries*, **22**, No. 3, 2009, pp. 353-359.

[8] Makarov D. and Molkov V., Plane Hydrogen Jets, *International Journal of Hydrogen Energy*, **38**, No. 19, 2013, pp. 8068-8083.

[9] Veser A., Kuznetsov M. and Fast G. et al., The Structure and Flame Propagation Regimes in Turbulent Hydrogen Jets, *International Journal of Hydrogen Energy*, **36**, No. 3, 2011, pp. 2351-2359.

[10] Friedrich A., Breitung W. and Stern G. et al., Ignition and Heat Radiation of Cryogenic Hydrogen Jets, *International Journal of Hydrogen Energy*, **37**, No. 22, 2012, pp. 17589-17598.

[11] Klinge F., Kirmse T. and Kompenhans J., Application of Quantitative Background Oriented Schlieren (BOS): Investigation of a Wing Tip Vortex in a Transonic Windtunnel, Pacific Symposium on Flow Visualization & Image Processing. DLR, 2003.

[12] Xiao J., Travis J. R. and Royl P. et al., Three-dimensional All-speed CFD Code for Safety Analysis of Nuclear Reactor Containment: Status of GASFLOW Parallelization, Model Development, Validation and Application, *Nuclear Engineering and Design*, **301**, 2016, pp. 290-310.

[13] Xiao J., Kuznetsov M. and Travis J. R., Experimental and Numerical Investigations of Hydrogen Jet Fire in a Vented Compartment, *International Journal of Hydrogen Energy*, **43**, No. 21, 2018, pp. 10167-10184.

[14] Li Y., Xiao J. and Zhang H. et al., Numerical Analysis of Hydrogen Release, Dispersion and Combustion in a Tunnel with Fuel Cell Vehicles Using All-speed CFD Code GASFLOW-MPI, *International Journal of Hydrogen Energy*, **46**, No. 23, 2021, pp. 12474-12486.

[15] Hirt C. W., Amsden A. A. and Cook J. L., An Arbitrary Lagrangian-Eulerian Computing Method for All Flow Speeds, *Journal of Computational Physics*, **14**, No. 2, 1974, pp. 227-253.

[16] Launder B. E. and Spalding D. B., The Numerical Computation of Turbulent Flows, *Computer Methods in Applied Mechanics and Engineering*, **3**, No. 2, 1974, pp. 269-289.

[17] Mller C., Hughes E. D. and Niederauer G. F. et al., GASFLOW: A Computational Fluid Dynamics Code for Gases, Aerosols, and Combustion, Volume 2: User's Manual, Office of Scientific and Technical Information Technical Reports, 1998.

[18] Magnussen B. F. and Hjertager B. H., On Mathematical Modeling of Turbulent Combustion with Special Emphasis on Soot Formation and Combustion, *Symposium on Combustion*, **16**, No. 1, 1977, pp. 719-729.

[19] IGC Doc 75/01/E/rev. Determination of safety distances. European Industrial Gases Association.